Spectral and Angular Responses of High Sensitivity Refractive Index Sensors Based on Titanium Nitride

Junior Asencios[1], **Arturo Talledo**[1,*], **Brayan Atoccsa**[1], **Ruben Puga**[1], **Héctor Loro**[1], **and Ramiro Moro**[2]

[1]Sputtering Laboratory, Universidad Nacional de Ingeniería, Av. Tupac Amaru 210, Lima, Peru
[2]Tianjin International Center for Nano Particles and Nano Systems, Tianjin University, 300072, China

Abstract— Refractive index sensors of high sensitivity were built by depositing thin films of titanium nitride and plane waveguides made of Nb_2O_5 and SiO_2 on the planar face of D-shaped prisms, by dc and rf magnetron sputtering. Devices with structures Glass/TiN, Sapphire/TiN and Sapphire/TiN/SiO_2/Nb_2O_5 were studied. Measurements of reflectance as a function of the angle of incidence were made in the Kretschmann configuration. For devices Glass/TiN and Sapphire/TiN, typical broad absorption band was observed. For devices with structure Sapphire/TiN/SiO_2/Nb_2O_5, we observed a sharp reflectance peak, at a very well defined value of the angle of incidence within the broad absorption band, attributed to the phenomena of Plasmon Induced Transparency (PIT) and Fano resonance. Then, in the range of incidence angle values for which PIT and Fano resonance were observed, we studied the spectral response in the range of wavelength between 400 and 800 nm. Results show that high sensitivity sensors may also be used as tunable-by-incidence-angle optical filters. All data, reflectance vs angle of incidence and reflectance vs wavelength, were fitted by using a calculation program based on the solutions to Maxwell equations and boundary conditions.

1. INTRODUCTION

Refractive Index Sensors (RISs) based on the phenomenon of Surface Plasmon Resonance (SPR) have been developed [1, 2] since the 1980's. Their main applications are in gas detection and in Biology, they are used extensively to determine association and dissociation kinetics, protein-ligand, protein-protein, or nucleic acid hybridization interactions. The Physics behind these devices is the excitation and detection of Surface Plasmon Polaritons (SPPs) in a metal-dielectric interface and the dependence of the maximum-absorption wave vector with the variation of the refractive index of the dielectric medium.

The first generation of refractive index sensors were constituted by a thin film of a noble metal (gold or silver) deposited on one surface of a prism. The experimental set up is similar to that used to study attenuated total reflection [3] and it is called Kretschmann configuration. For a characteristic range of incidence angle, greater than the critical angle, the evanescent wave excites oscillations of the electronic plasma of the metal film producing energy looses, and reflectance dips in reflectance-vs-angle-of-incidence data.

Other type of RIS were developed by overcoating the metal thin film with one dielectric layer. These are known as coupled plasmon-waveguide resonance (CPWR) spectroscopy [4].

More recently, since 2015, a new generation of RISs, that we call here high sensitivity refractive index sensors (HSRISs), comes being investigated based on the phenomenon of Plasma Induced Transparency and Fano resonance [5–9]. These devices consist on the overcoating of the metalic film with two layers of dielectric materials, one of low refractive index (L) and a second one of high refractive index (H). If we suppose that the refractive index of the investigated substance, placed on the top of the device, is lower than the H layer, we will have an LHL dielectric structure coated onto the metal film, i.e., we have the structure of a planar waveguide. When the device is set in the Kretscmann configuration, there exists a very well defined angle, greater than the critical angle, at which a mode of planar wave guide is excited. At this specific angle, the evanescent wave jumps toward the dielectric structure and no SPPs are excited on the metal film, obtaining then an extremely sharp peak of maximum reflectance within the absorption range. This sharp peak depends strongly of the refractive index of the investigated substance.

In this paper we report: (i) the experimental building of HSRISs by using a thin film of titanium nitride instead of the metallic thin film. (ii) the behaviour of the reflectance by a HSRIS based on titanium nitride when working in the Kretschmann configuration we use a fix wavelength laser and vary the angle of incidence and (iii) The spectral analysis of reflected ray when we use a source of white light and fix an angle of incidence with value greater than the critical angle.

*Corresponding author: Arturo Talledo (atalledo@uni.edu.pe).

2. MATERIALS AND STRUCTURE OF DEVICES

Figure 1 shows schematically the structure of the two types of sensors investigated in this work. The sensor represented in Figure 1(a) was built by depositing a titanium nitride film onto the planar surface of a D shaped prism. In Figure 1(b) we show the structure of a high sensitivity refractive index sensor; it was built by depositing onto the planar surface of a D-shaped prism successively one thin film of titanium nitride (approx. 35 nm), one layer of silicon dioxide (approx. 380 nm) and a layer of niobium pentoxide (approx. 140 nm).

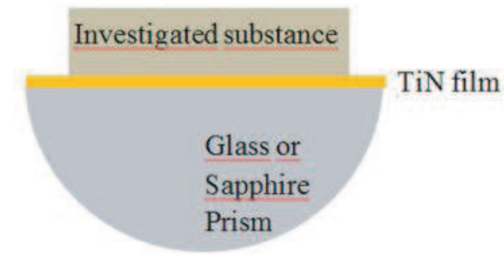

(a)

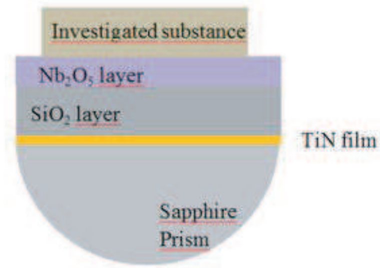

(b)

Figure 1: Schematic of (a) structure of SPR sensor which uses titanium nitride thin film instead of noble metal film, (b) high sensitivity refractive index sensor with a layer of silicon dioxide and a layer of niobium pentoxide deposited onto the TiN film.

Titanium nitride thin films were produced by dc magnetron sputtering onto the planar surface of D-shaped prisms made of glass or sapphire. The target was a 3 inches diameter and 4 mm-thick disk of metallic titanium, 99.99% pure. The process was achieved in an atmosphere of 92% argon +8% nitrogen. The plasma current was 400 mA and the deposition rate 20 nm per minute. The substrate temperature was 400°C during the deposition process. A second kind of samples were prepared depositing, onto the TiN thin film, a layer of silicon dioxide with thickness approximately 380 nm and a layer niobium pentoxide with thickness approximately of 140 nm; in such a way that we got a planar wave guide adjacent to the titanium nitride film. The SiO_2 layer was produced immediately after the titanium nitride film without opening the sputter chamber. The target was a silicon disk 3 inches diameter, 99.99% purity and 4 mm thick; the deposition atmosphere was 6% O_2 + 94% Ar and the deposition rate was one micron per hour. Deposition conditions for Nb_2O_5 films were similar to those of silicon dioxide but using a metallic target of niobium 99.99% pure.

X-ray diffraction was used for the verification of the crystalline structure of materials and Scanning Electron Microscopy (SEM) for verification of the structure of multilayers and measurement of their thickness. The instruments were Bruker D8 and Hitachi 8230, respectively. X-ray diffraction was achieved in the theta-2theta configuration with cooper radiation of wavelength 0.154 nm. Figure 1(a) shows a diffractogram of a thin film of titanium nitride on glass. In figure 1b we have a diffractogram of a bilayer, 45 nm-thick titanium nitride film and a 490 nm-thick layer of silicon dioxide. Samples were prepared at 300 and 400°C respectively. Typical diffraction peaks at 36.70 and 42.50 are observed which verify the structure of titanium nitride, rock salt structure with lattice parameter $a = 0.42$ nm. No diffraction peaks for silicon oxide layers tell us that they are amorphous. In Figure 3 we show the micrographic of system glass/TiN/SiO_2/Nb_2O_5.

3. MEASUREMENTS AND SIMULATION

The experimental set up for measurements of reflectance vs angle of incidence (angular response) in the Kretschmann configuration is schematically shown in Figure 4. The source was a helium-neon laser of 632,8 nm. A polarizer was placed between the laser and the prism in such a way that p-polarized light hits on the prism. The intensity of the reflected beam was measured by using a photoresistor, for angle values from 20 to 90° with one-degree intervals. In this work, we studied experimentally the ATR angle spectra for the two devices schematically shown in Figure 1.

The experimental set up for measurements of reflectance vs wavelength (spectral response) in the Kretschmann configuration is schematically shown in Figure 5. The source was a 50 W tungsten lamp. A polarizer was placed between the lamp and the prism in such a way that p-polarized light hits on the prism. The reflected beam was analyzed for wavelength values from 400 to 800 nm with two-nm intervals. A spectrophotometer B&W TEC model BTC_110 s grating 900 l/mm was used.

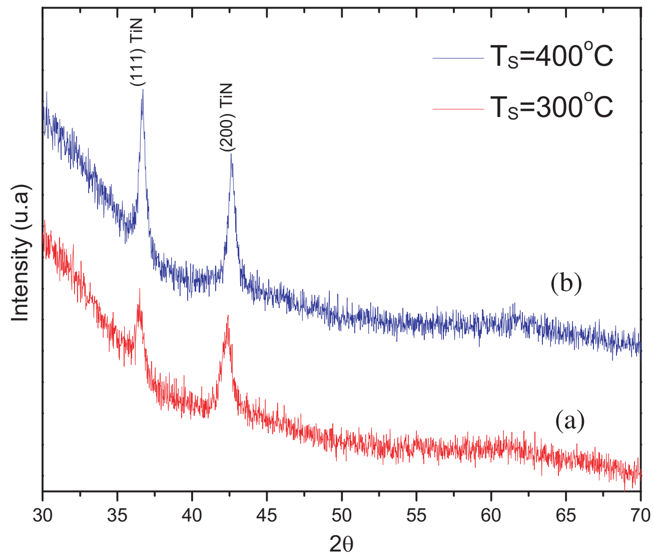

Figure 2: X-ray diffractograms of (a) Glass/TiN, (b) Glass/TiN/SiO_2.

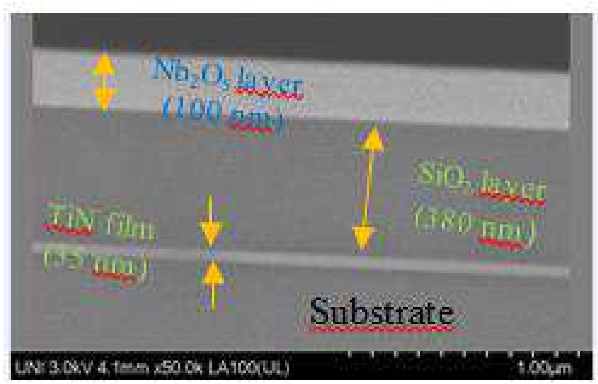

Figure 3: SEM Micrographic showing the cross-section of a system TiN/SiO_2/Nb_2O_5 deposited on glass; the thicknesses were 35 nm, 380 nm and 100 nm for TiN, SiO_2 and Nb_2O_5 films respectively.

In this work, we studied experimentally the spectral response for the device schematically shown in Figure 1(b).

The problem of calculating the Reflectance vs angle of incidence (angular response) in terms of the refractive indices (n_j) and thickness of the different layers (t_j) is a completely solved problem by the Electromagnetic Theory [10, 11]. The standard procedure to solve this problem consists in: (i) To propose functions which describe electric and magnetic fields in each medium; these functions, which describe p-polarized (or Transversal Magnetic) electromagnetic waves are solutions to Maxwell equations and the wave equation; they also satisfy boundary conditions for continuity of the fields H and E in each interface; relationship between fields at each side of an interface are the very well-known Fresnel coefficients. (ii) One 2×2 matrix is constructed which relates the incident and reflected waves in medium 1 (the prism) with the outgoing ray in the last medium (air, left side in all Figure 4); this matrix is expressed in terms of the incident angle, the refractive indices of all the media and the thickness of all the layers. Following these ideas, we made a program in JavaScript language which simulates the angular response, at a well-defined wavelength 633 nm), for each set of n_j and t_j parameters. This program also works inversely: when we have an experimental angle response, we can obtain the optical parameters (complex refractive index, in general, $n = n + ik$) and thicknesses t_j of the media which better fit the experimental data. In this work, we used the program in both senses: *simulation* for designing, before manufacturing the plasmonic structures and *fitting* after the measurements of reflectance vs angle of incidence. The program can be easily change to simulate and/or fit spectral response at a well-defined angle of incidence.

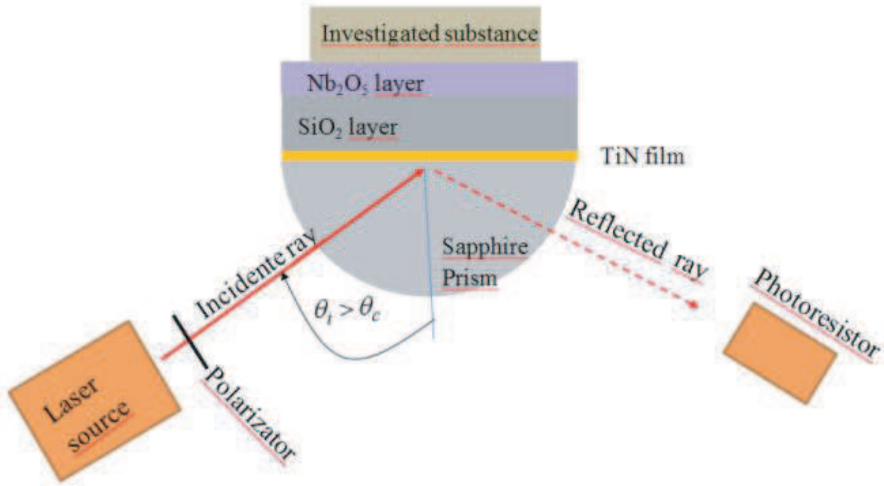

Figure 4: Schematic of the experimental setup for Reflectance vs Incidence Angle measurements.

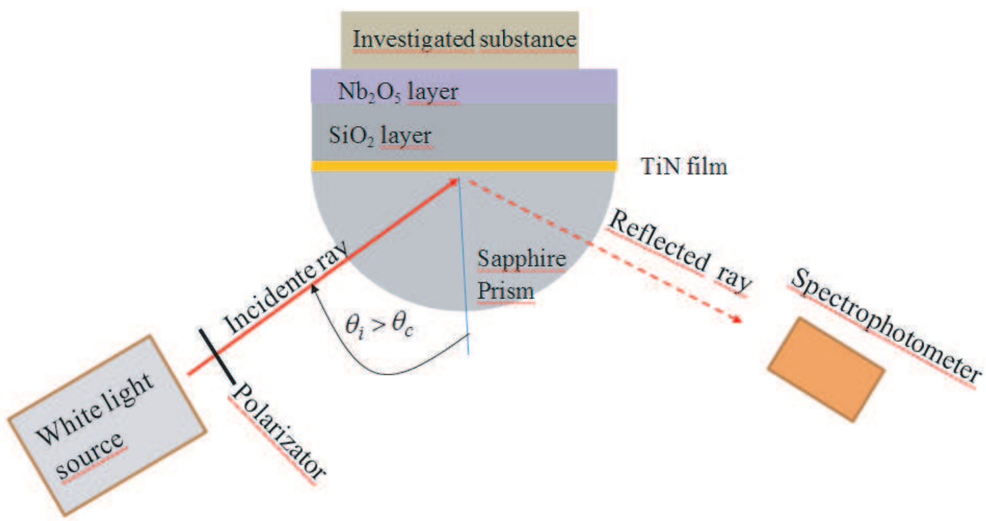

Figure 5: Schematic of the experimental setup for Reflectance vs wavelength measurements.

4. ANGULAR RESPONSE OF SPR SENSORS AND HIGH SENSITIVITY SENSORS

In this part of our work we studied the angular response, i.e., the reflectance-vs-angle-of incidence data, for two kind of devices (i) SPR sensors with structure described in Figure 1(a) and (ii) high sensitive refractive index sensors with structure described in Figure 1(b).

In Figure 6 we show the angular response for two spr sensors (i) one built by deposition of a thin film of titanium nitride onto the planar surface of a glass prism (red curve) and (ii) other built by deposition of a TiN thin film onto the planar surface of a sapphire prism (blue curve).

The main feature of these angular responses is a very wide absorption band going from the critical angle to incidence angle 80°. The minimum of reflectance was obtained for angles of incidence approximately 50° for samples made on glass prism. For samples made on sapphire prism the maximum absorption was at 45°. The full width at half height is approximately 35° for samples on glass prism and 25° for samples on the sapphire prism. The shift of the absorption curves is due to the difference on the refractive index of glass and sapphire. For glass $n = 1,5$; for sapphire $n = 1,77$. The difference on the width of the absorption band can be explained for the difference on the electrical conductivity of the titanium nitride thin film, expressed also as difference in the values the extinction coefficient k. For TiN on glass $k = 2.22$ for TiN on sappfire $k = 2.17$. These features of our data agree very well with those reported by N. C. Chen et al. [12].

In Figure 7 we show the angular response for one high sensitive refractive index sensor (i) when the investigated substance is air, $n = 1$ (red curve) and (ii) when the investigated substance is liquid silicone, $n = 1.48$ (blue curve).

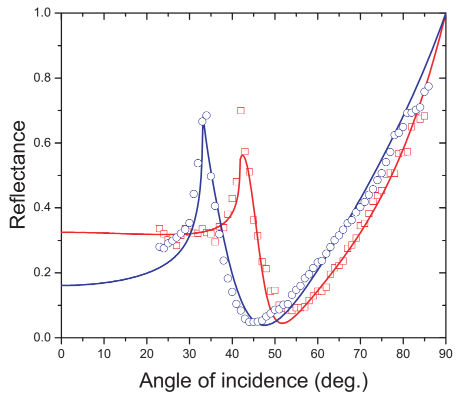

Figure 6: Experimental data and fitting curves of Reflectance vs angle of incidence for the system (a) glass/TiN, red curve and (b) Sapphire/TiN. blue curve.

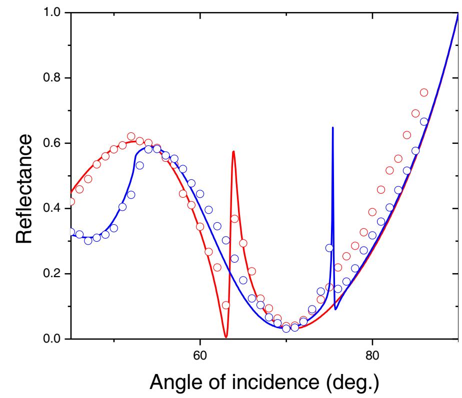

Figure 7: Experimental data and fitting curves of Reflectance vs angle of incidence for a HSRIS sensing (a) air ($n = 1$) red curve and (b) liquid silicone ($n = 1.48$), blue curve.

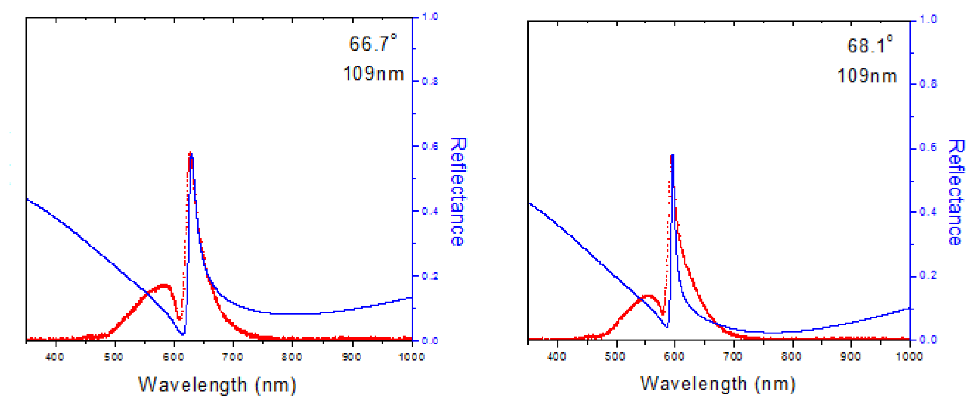

Figure 8: Experimental spectral response (red curves) and simulation (blue curves) of a high refractive index sensor with thickness of the niobium pentoxide $t = 109$ nm for the angles of incidence shown in the insets.

The main feature of these angular responses is the presence of a sharp peak of reflectance within a wide absorption band, strongly depending on the value of the refractive index of the investigated substance. The physics behind the behavior of these devices is the interaction between the plane waveguide traveling on the niobium pentoxide layer and the surface plasmon polariton traveling along the SiO_2/TiN interface. When the modal condition [11] for the propagation of a waveguide is satisfied, the evanescent wave jumps toward the non-dissipative pentoxide layer instead of traveling along the dissipative titanium nitride, avoiding excitation of surface plasmon polaritons and energy loss. The typical asymmetric curve (better observed in the red curve) superposed to the absorption band is attributed to the phenomenon known as Fano resonance [13]. This phenomenon is also associated with the Plasmon Induced Transparency and Electromagnetically induced transparency [5–9, 14, 15].

5. SPECTRAL RESPONSE OF HIGH SENSITIVITY SENSORS BASED ON TITANIUM NITRIDE

In this section we report the spectral response for two HSRISs in the Kretschmann configuration. The structure of devices is that of Figure 1(b), i.e., Sapphire/TiN/SiO_2/Nb_2O_5. The thicknesses of the TiN thin film and the SiO_2 layer were 35 nm and 380 nm, were for both samples. The thickness of the Nb_2O_5 was i) $t = 109$ nm and ii) $t = 139$ nm. The experimental set up was that shown in Figure 3. Figure 8 shows the spectral reflectance for the HSRIS with t = 109 nm with angles of incidence: a) 66.7° and b) 68.1°. Figures 9 shows the spectral reflectance for the HSRIS with $t = 139$ nm with angles of incidence: 71.4°, 73.1° and 76.6°. In all cases the sensing substance was liquid silicone with refractive index $n = 1.48$.

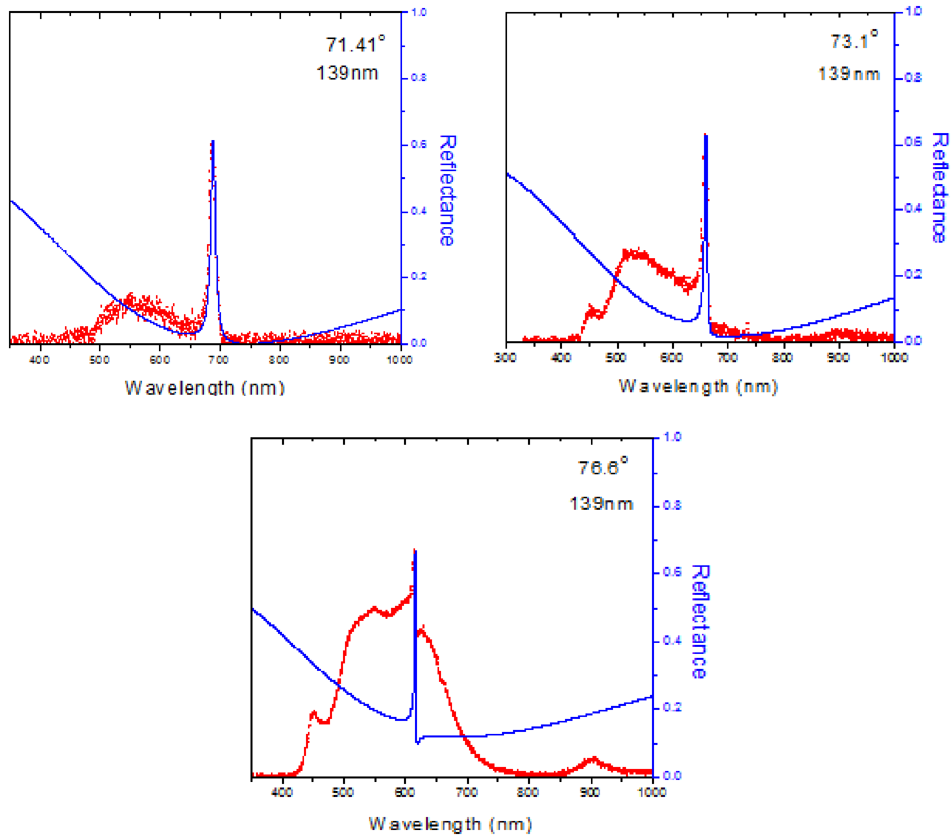

Figure 9: Experimental spectral response (red curves) and simulation (blue curves) of a high refractive index sensor with thickness of the niobium pentoxide $t = 139\,\text{nm}$ for the angles of incidence shown in the insets.

6. SIMULATING PRACTICAL APPLICATIONS

In order to determine the potential sensitivity of the HSRISs reported in this paper, in this section we show simulations of angular response and spectral response for hypothetical samples with refractive index $n = 1.33$ and $n = 1.34$. For these simulations we used the data of the substrate and films which make up the devices described in this paper. Refractive indices of sapphire, titanium nitride, silicon dioxide and niobium pentoxide are respectively: 1.77, $0.9 + 2.2\text{i}$, 1.46 and 2.2. The thickness values of the TiN, SiO_2 and Nb_2O_5 films are respectively: 35 nm, 380 nm and 109 nm. For angle-response simulations we used laser wavelength 633 nm.

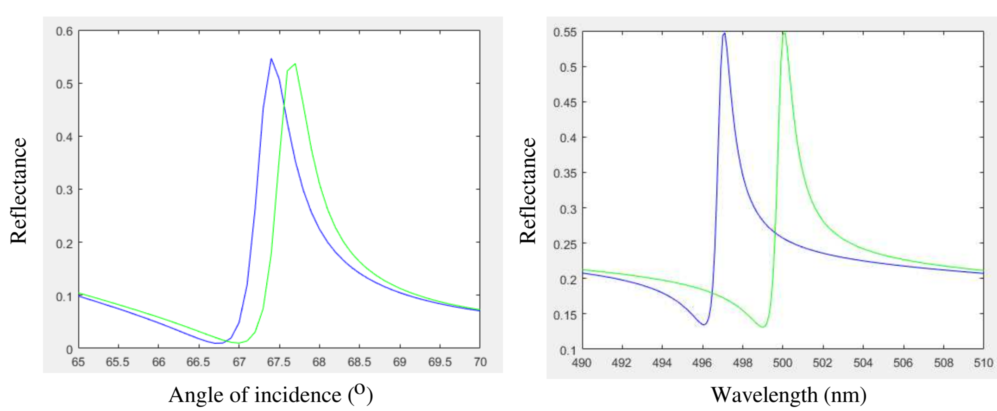

(a) (b)

Figure 10: Simulation of (a) angular response and (b) spectral response of HSRISs for sensing hypothetical samples with $n = 1.33$ (blue curves) and $n = 1.34$ (green curves).

7. CONCLUSIONS

High sensitivity refractive index sensors were built by depositing thin films of titanium nitride, silicon dioxide and niobium pentoxide onto the planar surface of D-shaped prism made of sapphire. Angular response was studied in the range 20°–90° and the more relevant feature is the presence of a very sharp reflectance peak within the wide absorption band typical of the surface plasmon resonance of devices coated only with titanium nitride films. The angle of incidence at which sharp reflectance peaks are obtained varies between 65° and 75°, depending of the thickness of the niobium pentoxide layer and the refractive index of the investigated substance. Then the spectral response was studied by maintaining fix the angle of incidence at values between 65° and 75°. The spectral response show sharp reflectance peaks at very well defined wavelength values which vary with the angle of incidence; these results suggest that these HSRISs can also be used as tunable optical filters. In all cases there is reasonable agreement between experimental results and respective simulations. With the data of thickness and refractive index of the films which make up our devices, we made simulations which show that for hypothetical investigated substances with refractive index $n = 1.33$ and $n = 1.34$, the variation of the angle of incidence needed for sharp peaks would be 0.3°. On the other hand, by using these data of our HSRISs in the simulation of the spectral response, for the variation of the refractive index between 1.33 and 1.34 of the investigated substance, we would have a variation of 3 nm in the wavelength value of the reflectance peak.

ACKNOWLEDGMENT

One of us, J. A., is very grateful to Concytec for scholarship financing doctoral studies. A. T. is also very grateful to Universidad Nacional de Ingeniería and MINEDU Perú for special grants as a researcher professor.

REFERENCES

1. Nylander, C., B. Liedberg, and T. Lind, *Sensors and Actuators*, Vol. 3, 79–88, 1982/1983.
2. Liedberg, B., C. Nylander, and I. Lunstrom, *Biosensors & Bioelectronics*, Vol. 10, i–ix, 1995.
3. Erwin Kretschmann, Z., *Physik*, Vol. 241, 313–324, 1971.
4. Salamon, Z., H. A. Macleod, and G. Tollin, *Biophysical Journal*, Vol. 73, 2791–2797, 1997.
5. Hayashi, S., D. V. Nesterenko, and Z. Sekkat, *J. Phys. D: Appl. Phys.*, Vol. 48, 325303, 2015.
6. Hayashi, S., D. V. Nesterenko, and Z. Sekkat, *Applied Physics Express*, Vol. 8, 022201, 2015.
7. Nesterenko, D. V., S. Hayashi, and Z. Sekkat, *J. Opt.*, 18, 2016.
8. Hayashi, S., D. Nesterenko, A. Rahmouni, and Z. Sekkat, *Appl. Phys. Lett.*, Vol. 108, 051101, 2016.
9. Sekkat, Z., S. Hayashi, D. V. Nesterenko, A. Rahmouni, S. Refki, H. Ishitobi, Y. Inouye, and S. Kawata, *Optics Express*, Vol. 24, No. 18/5, 20080, 2106.
10. *Thin Films Optical Filters*, 4th edition, H. Angus Macleod, CRC Press, 42–46, 2010.
11. *Óptica Electromagnética Vol. II Materiales y Aplicaciones*, José Manuel Cabrera, Fernando Agulló López, Fernando Jesús López, Addison Wesley/Universidad Autónoma de Madrid, Madrid, Spain, 209–259, 2000.
12. Chen, N. C., W. C. Lien, C. R. Liu, Y. L. Huang, Y. R. Lin, C. Chou, S. Y. Chang, and C. W. Ho, *Journal of Applied Physics*, Vol. 109, 043104, 2011.
13. Fano, U., *Physical Review*, Vol. 124, No. 6, 1866–1878, 1961.
14. Boller, K.-J., A. Imamoglu, and E. S. Harris, *Physical Review Letters*, Vol. 66, No. 20, 2593–2596, May 1991.
15. Harris, S. E., *Phys. Today*, Vol. 50, No. 7, 36, 1997.